

Application of Magnification Control for the Neural Gas Network in a Sensorimotor Architecture for Robot Navigation*

Thomas Villmann^{+†} and Andrea Heinze[°]
⁺University Leipzig, Clinic for Psychotherapy
Augustusplatz 10/11 04107 Leipzig, Germany
[°]Ilmenau Technical University
Department of Neuroinformatics
email: villmann@informatik.uni-leipzig.de

Abstract

In the present article we consider the influence of the control of the magnification in a Neural Gas Network (NG). The NG is embedded in a sensorimotor architecture of a robot navigation system and serves as a classifier for the sensory system states. This representation and learned connections within this architecture contribute to movement decisions concerning the system's goals. Hence, a faithful clustering of the sensory inputs directly influences the quality of resulting behavior. To improve the performance of the NG we extended the algorithm by a magnification control scheme. It places special emphasis on rarely occurring but relevant sensory inputs requiring careful control. We show the performance improvement for the robot system achieved by this strategy.

1 Introduction

Neural maps are a widely applied type of neural vector quantizers which are used for example in data visualization, feature extraction, principle component analysis, image processing, classification tasks, and robotics [6]. Several models have been introduced; probably the best known of them was developed by KOHONEN. A further well studied approach is that of the Neural Gas Network (NG) proposed by MARTINETZ [15].¹

In robotic applications (neural) vector quantizers often are used to classify and determine the state of the system [19], [22]. Based on the classification result, a subsequent motor action is selected. Hence, a faithful representation of the state space \mathcal{S} of the system is required for optimal robot navigation. In particular, critical, e.g. dangerous states have to be controlled carefully. However, the frequency of such critical situations typically is low in comparison to safe states. This results in an inhomogeneous probability density P of \mathcal{S} . Moreover, the density P is low in regions of critical system states. Usually, the vector quantizers distributes the nodes (neurons) according to P and, hence, the neural vector quantizer will allocate only a

*This work was supported by the DFG-Grants Gr 1378/1-1&2 to H.-M. Gross and by DFG Graduiertenkolleg GK 164

[†]*corresponding author*

¹In the area of neural maps it was extended to the method of topology preserving mapping called Topology Representing Network (TRN) [14].

few neurons to these space regions. This contradicts the desired careful control [3]. Therefore it is necessary to add some mechanisms to influence the distribution of the neurons which is related to the problem of so-called magnification control.

In the present paper we consider a real world robot environment. Here the vector quantizer works as a classifier system as proposed above. In our studies we investigated the performance change of the robot system arising from magnification control in the neural vector quantizer. The NG network was used because of its theoretically well founded behavior.

The paper is organized as follows. In section 2 we describe the robot system architecture and the role of the vector quantizing module. After this in section 4 we briefly summarize the NG and its properties and highlight recent developments in magnification control of NG. The application results are presented in section 5 and some remarks and discussion conclude the article in section 6.

2 Architecture of the sensorimotor system

Based on findings for the sensorimotor character of perception [1, 17], we have developed an alternative approach to perception that avoids the common separation of perception and generation of behavior and fuses both aspects into a consistent neural process [16, 5]. In this approach, perception of space and shape in the environment is regarded to be an active process which anticipates the sensory consequences of alternative hypothetical interactions with the environment initiated by the sensorimotor system, starting from the current sensory situation. In the following, we briefly present the developed architecture for a local navigation which serves as a frame for the investigations focusing on the two aspects of representation of sensorimotor situations and the generation of behavior. This paper especially emphasizes the investigation of representing sensorimotor situations and their results. A detailed discussion of the capability of the biologically motivated computational model to anticipate and evaluate hypothetical sensorimotor sequences is presented in [5] and [7].

2.1 Experimental Framework

Observable behaviors are the only indicators to evaluate and compare the perceptual performance of sensorimotor systems as a whole. Therefore, we investigate our sensorimotor concept within the framework of a simple local navigation behavior by a real Khepera robot pursuing the goals of obstacle avoidance and fast and straight movement. The visual sensory inputs necessary for interaction with the robot's nearby environment were provided by an omnicaamera. Given the tasks of obstacle avoidance and purposeful locomotion, it supplies a wealth of information.

As an alternative to the camera with the image processing involved, and in fact a common choice, Khepera offers infrared (IR) sensors. Unfortunately, these are of very limited utility due to their noisy, inconsistent readings and operation only in short range which makes it very hard still to manage to avoid an obstacle once it could be detected.

To take advantage of its benefits we use the omnidirectional camera to generate sensory inputs. A number of transformations of the image from the omnicaamera furnish the visual input features for our architecture. The first is a polar transformation, followed by a transformation into a physiological color space [18] which generates decorrelated maps for color and intensity. The importance of the latter is obvious for real environments where white background and yellow obstacles must be distinguished. 8 receptive fields of different, hand-crafted size of the color mean are formed from the Blue-Yellow map. These receptive fields yield a good recognition and localization of those obstacles relevant for the behavior of the Khepera, while those behind or to the sides of the robot, with lower relevance, are recognized, but not localized exactly.

2.2 Sensorimotor Representation of Situations

The architecture is composed of sensorimotor assemblies of processing nodes (see figure 1). It accomplishes a parallel generation of sequences of sensorimotor hypotheses, realized by a spread of activity through the connections between the nodes within this model. These connections, thus, allow the direct prediction of subsequent sensorimotor situations as well as an evaluation (w^r) and competence (w^c) for each transition.

For learning within the sensorimotor architecture, special attention must be paid to the representation of the sensorimotor situations and the learning of competence and evaluation weights for transitions between subsequent sensorimotor states. In our investigations, we used a Neural Gas [13] and two magnification controlled Neural Gas networks for clustering of the sensory situations.

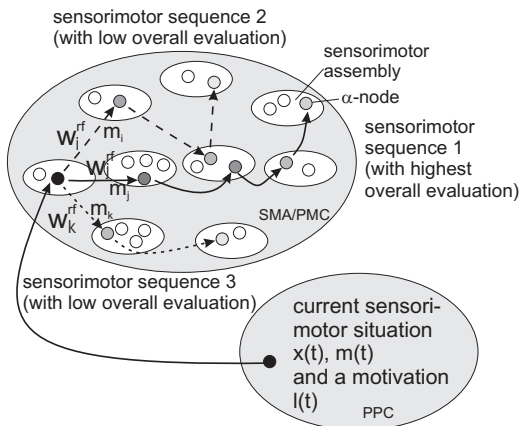


Figure 1: Basic structure of the architecture. Each node encodes a sensory situation specified by the motor context that resulted in the respective sensory situation. This figure schematically illustrates three short sequences. Each of the generated sequences may have a different length and cumulative evaluation. The connections between the nodes encode the motor commands (m) along with their evaluations (w^r) and competence (w^c) for the corresponding sensorimotor transition.

The nodes in each sensorimotor assembly represent alternative motor commands serving to bring the system into the respective sensory situation. Thus, initiated by a real sensorimotor situation, a certain node in our model is activated which propagates its activity to all other nodes connected to it by corticocortical connections. The hereby activated nodes may in turn activate further nodes, thus generating whole sequences of sensorimotor hypotheses.

During the parallel generation of sequences of sensorimotor hypotheses, the model assumes that the selection of the best evaluated sequence is realized by the cumulation and backpropagation of the activity of the nodes of each sequence [7]. We omit the details of the generation of sequences as they are irrelevant in this context and concentrate on an appropriate clustering of relevant sensory situations.

3 Magnification control of the Neural Gas Network

As mentioned in the introduction, different types of (neural) vector quantizers can serve as classifier systems for the analysis of the present state in sensorimotor control. Neural approaches often achieve better performance because of their adaptive nature. Moreover, the adaptability introduces the possibility of retraining. Among the neural quantizers the NG plays an outstanding role. An important advantage of the NG are the adaptation dynamics of the weight vectors which follow a potential minimizing procedure [15]. It avoids the vector quantization problems inherent to self-organizing map (SOM) [11]. After a short introduction of the NG we address the problem of magnification control.

3.1 The Neural Gas Network

The NG maps data vectors \mathbf{v} from a possibly high-dimensional data manifold $\mathcal{S} \subseteq \mathbb{R}^d$ onto a set A of neurons i which is formally written as $\Psi_{\mathcal{S} \rightarrow A} : \mathcal{S} \rightarrow A$. Each neuron i is associated

with a pointer $\mathbf{w}_i \in \mathfrak{R}^d$ all of which establish the set $\mathbf{W} = \{\mathbf{w}_i\}_{i \in A}$. The mapping description is a winner take all rule, i.e. a stimulus vector $\mathbf{v} \in \mathcal{S}$ is mapped onto the neuron $s \in A$ whose the pointer \mathbf{w}_s is closest to the actually presented stimulus vector \mathbf{v} ,

$$\Psi_{\mathcal{S} \rightarrow A} : \mathbf{v} \mapsto s(\mathbf{v}) = \underset{i \in A}{\operatorname{argmin}} \|\mathbf{v} - \mathbf{w}_i\| . \quad (3.1)$$

The neuron s is called *winner neuron* or *best-matching unit*. The set

$$R_j = \left\{ \mathbf{v} \in \mathcal{S} \subseteq \mathfrak{R}^d \mid j = \Psi_{\mathcal{S} \rightarrow A}(\mathbf{v}) \right\} \quad (3.2)$$

forms the (masked) receptive field of the neuron j .²

During the adaptation process a sequence of data points $\mathbf{v} \in \mathcal{S}$ is presented to the map drawn from the stimuli distribution $P(\mathcal{S})$. Then the currently most proximate neuron s according to (3.1) is determined, and the pointer \mathbf{w}_s as well as all pointers \mathbf{w}_i of neurons in the neighborhood of s are shifted towards \mathbf{v} , according to

$$\Delta \mathbf{w}_i = \epsilon h_\lambda(i, \mathbf{v}, \mathbf{W})(\mathbf{v} - \mathbf{w}_i) . \quad (3.3)$$

The property of “being in the neighborhood of s ” is represented by a neighborhood function $h_\lambda(i, \mathbf{v}, \mathbf{W})$. The neighborhood function for the NG is defined as

$$h_\lambda(i, \mathbf{v}, \mathbf{W}) = \exp\left(-\frac{k_i(\mathbf{v}, \mathbf{W})}{\lambda}\right) \quad (3.4)$$

where $k_i(\mathbf{v}, \mathbf{W})$ defines the rank of neighborhood, i.e. the number of pointers \mathbf{w}_j for which the relation $\|\mathbf{v} - \mathbf{w}_j\| \leq \|\mathbf{v} - \mathbf{w}_i\|$ is valid [15], especially we have $h_\lambda(s, \mathbf{v}, \mathbf{W}) = 1.0$. We remark that in contrast to the SOM the neighborhood function is evaluated in the input space. Moreover, the adaptation rule for the weight vectors in average follow potential dynamics with

$$E(\mathbf{w}, \lambda) = \frac{1}{2C(\lambda)} \sum_{i=1}^N \int P(\mathbf{v}) \cdot h_\lambda(i, \mathbf{v}, \mathbf{W}) \cdot (\mathbf{v} - \mathbf{w}_i)^2 d\mathbf{v} \quad (3.5)$$

as the respective energy function, with $C(\lambda) = \sum_{i=1}^N h_\lambda(i, \mathbf{v}, \mathbf{W})$ a normalization constant.

4 Magnification, magnification control and optimal learning in the NG

The *magnification* of the final trained map reflects the relation between the data density $P(\mathcal{S})$ and the density ρ of the weight vectors. For the NG the relation

$$P(\mathcal{S}) \propto \rho(\mathbf{w})^\alpha \quad (4.1)$$

with $\alpha = \frac{d}{d+2}$ was derived [15]. The exponent α is called *magnification factor*. It depends on the dimensionality of the input space embedded in \mathfrak{R}^d . The information transfer, in general, is not independent from the magnification of the map [23]. It was derived that for a vector quantizer³ realizing an optimal information transfer, the relation $\alpha = 1$ holds. It is related to a maximum of the entropy

$$H = - \sum_{i=1}^N p_i \cdot \log(p_i) \quad (4.2)$$

²In contrast to the SOM [11], in the TRN the neurons are not arranged on a priori fixed grid. The topological structure of A itself is subject to learning [14].

³or a neural map in our context

whereby p_i is the probability that the neuron i is the winner [2],[6].⁴ On the other hand, a vector quantizer minimizes the mean distortion error

$$E_\xi = \int_{\mathcal{S}} \|\mathbf{w}_s - \mathbf{v}\|^\xi P(\mathbf{v}) d\mathbf{v} \quad (4.3)$$

if for the magnification factor $\alpha = \frac{d}{d+\xi}$ with $\mathbf{v} \in \mathcal{S} \subseteq \mathfrak{R}^d$ [23] is valid. Hence, the usual NG minimizes the usual E_2 distortion error.

Consequently, the question is, how one can impact the magnification factor to achieve an *a priori* chosen optimization goal, i.e. an *a priori* chosen magnification factor. Several approaches are established for equiprobabilistic vector quantizers (for an overview we refer to [10]). In the present application the magnification control is achieved by modified weight adaptation which now reads as

$$\Delta \mathbf{w}_i = \epsilon_{s(\mathbf{v})} h_\lambda(i, \mathbf{v}, \mathbf{W}) (\mathbf{v} - \mathbf{w}_i) \quad (4.4)$$

now using a local learning rate $\epsilon_{s(\mathbf{v})}$ [9] and $s(\mathbf{v})$ is the best-matching neuron with respect to (3.1). Therefore, we have to specify the choice of the now *local* learning parameters $\epsilon_i = \epsilon(\mathbf{w}_i)$ of a neuron i . The most convenient approach is that the local learning parameters $\epsilon_i = \epsilon(\mathbf{w}_i)$ depend on the stimulus density P at the position of their weight vectors \mathbf{w}_i via

$$\langle \epsilon_i \rangle = \epsilon_0 P(\mathbf{w}_i)^m \quad (4.5)$$

where the brackets $\langle \dots \rangle$ denote the average over time. The new parameter m is an additional one to the usual parameters ϵ_0 and λ of the NG-algorithm. Other approaches are discussed in [21] and [10]. The consideration of the resulting dynamics yields

$$\rho(\mathbf{W}) \propto P(\mathbf{W})^{a'} \quad (4.6)$$

with

$$a' = \alpha \cdot (m + 1) \quad (4.7)$$

Here we emphasize that the derivation of the magnification factor is determined, in contradiction to the SOM, for an arbitrary dimension d of the input space [20].

For applications the equation (4.5) for $\epsilon_s(t)$ is not practicable because of the usually unknown probability density P . To overcome this problem the information already acquired by the network is used for realizing the learning rule (4.4):

$$P(\mathbf{w}_i) \propto p_i \rho(\mathbf{w}_i) \quad (4.8)$$

where $\rho(\mathbf{w}_i)$ is the receptive field density and p_i is the probability that the neuron i is the best-matching one in the sense of (3.1). Using this approach, the relation (4.5) is approximated by

$$\epsilon_s(t) = \epsilon_0 \left(\frac{1}{\Delta t_s} \left(\frac{1}{\|\mathbf{v} - \mathbf{w}_s\|^{d_{\text{eff}}}} \right) \right)^m \quad (4.9)$$

with s being the best-matching neuron for the present stimulus \mathbf{v} and Δt_s the difference between the present value of t and that of the last instance, when the considered neuron won the competition (3.1) following the approach in [8]. $\frac{1}{\Delta t_s}$ approximates the winner probability p_i in equation 4.8, and the fraction $\frac{1}{\|\mathbf{v} - \mathbf{w}_s\|^{d_{\text{eff}}}}$ determines the receptive field density $\rho(\mathbf{w}_i)$. In equation 4.9 d_{eff} gives the intrinsic dimension of the state space \mathcal{S} which can be approximated by the Grassberger-Procaccia-dimension d_{GP} [4] In addition, we prespecified an upper bound ϵ_{max} .

⁴A neural network which generates such optimal maps is the network of LINSKER [12] mentioned above.

5 Application results in the experimental environment

5.1 Sensory clustering

After generation of visual inputs as explained in section 2.1, these were clustered by a normal NG and two NG featuring magnification control. In all exemplary cases in figure 2, a separate network with 30 sensorimotor assemblies was trained with inputs gathered from random motor commands for 117210 training steps for the NG and the magnification controlled NG (mcNG1). The difference between mcNG1 and the second magnification controlled NG (mcNG2) is only the number of training steps, 390700 for mcNG2, because a magnification controlled NG requires more training steps than a regular one due to one more free parameter.

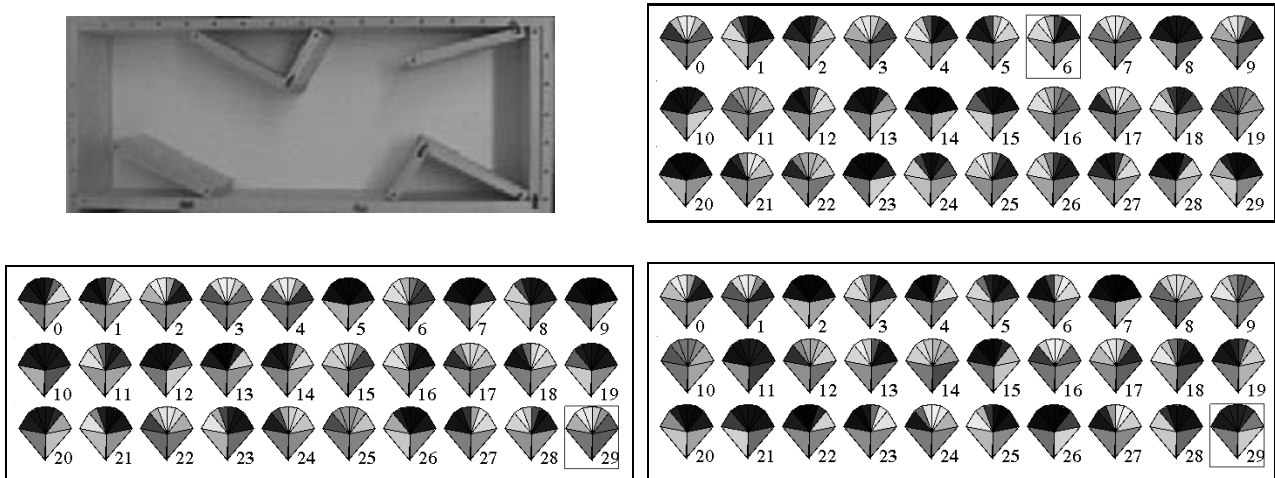


Figure 2: Different clusterer configurations produce different sensory representations. The sensory situations of the scenario (**upper left**), were clustered by a NG (**upper right**), a magnification controlled NG (mcNG1, 117210 training steps, **lower left**) and a magnification controlled NG (mcNG2, 390700 training steps, **lower right**). Situations are obtained from the 8 values of the receptive fields of different size resulting from the omnidirectional camera image. 4 small receptive fields in front of the robot yield an accurate description of the position of obstacles in front, while the larger receptive fields on the sides and the back yield only information about the existence of obstacles. The 8 weight values of each represented sensory situation (neuron) are depicted by an octagon, where the size of the triangle codes the size of the receptive field represented. The gray value within the triangle represents the value of the weight. Dark triangles represent an obstacle and light ones free space, such that neuron 20 of the regular NG (**upper right**) codes a situation in front of a wall.

As mentioned in the introduction the goal is to improve the navigation behavior of the robot. To achieve an improvement we now applied the magnification control scheme in our architecture. We are interested in a maximal mutual information to obtain an optimal information flow from the sensors to the control unit which, finally, should yield a higher performance. Hence, a maximization of the entropy is required which corresponds to a magnification factor $\alpha' = 1$. For this purpose the Grassberger-Procaccia-dimension d_{GP} was determined to estimate the respective m -values in the magnification control scheme (4.9). After the network training procedures the entropy H of several network configurations and learning environments was computed as a first quality measure according to which should have a maximum for the magnification factor $\alpha' = 1$, i.e. for the controlled maps the entropy value should be higher than the uncontrolled value. Furthermore, we remark that in the case of an ideal mapping $H_{\max}^N = -\sum_{i=1}^N \frac{1}{N} \cdot \log\left(\frac{1}{N}\right) = \log\left(\frac{1}{N}\right)$ holds, which yields $H_{\max}^{30} = 3.401$. The obtained entropy values are depicted in table 1.

The corresponding neuron weights for these clusterer configurations are visualized in figure 2. The results show a strong improvement, the entropies of the controlled NG are very close to the optimal one. Moreover an extremely long learning does not lead to any further significant improvements due to the control scheme.

N - number of neurons	training steps	entropy resulted from usual NG	entropy resulted from controlled NG
30	117210	3.15502	3.373282
30	390700		3.388126

Table 1: Entropy for different time scales for NG with and without magnification controlled NG in the scenario with obstacles

The clusterer results provided in figure 2 demonstrate that mcNG1 and the mcNG2 produce different sensory representations than a usual NG. All clusterers capture important situations of the scenario as exemplified by figure 2 (in front of a wall: NG sensorimotor assembly 8 and mcNG2 sensorimotor assembly 7; or in the middle between two obstacles: NG sensorimotor assembly 0 and mcNG2 sensorimotor assembly 16). However, it is impossible to evaluate the utility of those representations with respect to learnable motor commands only visually with figures such as figure 2 or by formal entropy ranking.

5.2 Behavior

An evaluation of the learned sensory representations can only be realized by judging the resulting learnable behavior. Therefore, both sensory representations were used for a training of sensorimotor transitions between nodes to obtain knowledge about behaviors.

Each of the 30 sensorimotor assemblies of all three clusterers was supplied a number of nodes, representing one motor command each (see figure 1). To simplify the investigations, only three motor commands were used (go left ahead $\phi = -12^\circ$, $s = 2.1cm$, go straight ahead $\phi = 0^\circ$, $s = 2.1cm$, go right ahead $\phi = 12^\circ$, $s = 2.1cm$).

After learning the structure of the sensory situations, each system (NG, mcNG1 and mcNG2) was presented the same test set containing 19.535 patterns of random sensorimotor transitions to train the connections w^r and w^c between nodes (for details concerning the training, see [7]). After that, each map was allowed to train for another 6.000 steps utilizing either exploration⁵ or reactive action selection⁶.

Investigations regarding a comparison of the behavior using a NG, mcNG1 and mcNG2 are shown in figure 3. Beginning from two scenario positions left and right in the scenario, the trials ended by a collision or at the respective other end of the scenario. The Khepera was tracked during all investigations by a top view camera and the evaluation signal obtained for each step was recorded.

Our investigations show that all systems are able to navigate without collisions in safe situations such as between obstacles or free space (not depicted). The evaluation signals in figure 3 reveal, that the system with the normal NG starts its avoidance motions too late when approaching the obstacle and starting from the right starting point. The first avoidance motion is executed in step 11 (from start), while the system with mcNG1 starts avoiding in step 7 (cf. figure 3 middle). Since both systems experienced the same training and were able to adapt their competence and

⁵In each situation, the motor command visited least often is selected.

⁶In each situation, the motor command is selected that brings the system into the subsequent situation with the highest evaluation depending on a calculation involving the competence and the evaluation weights.

evaluation weights for a sufficient amount of time, it is safe to assume that the difference in their behavior is caused by the different sensory representations.

Another example for the problem of sensory representation is visible in the behavior produced by mcNG2 (figure 2 right). Starting from the right starting point in the scenario, the sensorimotor assemblies representing a situation between two obstacles are activated during the first five steps. Although already now both the normal NG and mcNG1 are able to represent the approaching wall on the right, mcNG2 does not have a sensorimotor assembly representing this situation and, uses an assembly representing free space during the following three steps. This representation is the reason that mcNG2 is too late to initiate an avoidance movement as visible in the evaluation signals. This problem could be caused by using too few neurons. The number of neurons must be limited due to finite computational resources, especially the need to store the sensorimotor transitions between the neurons.

In general, we have found that the motion behavior is improved if the controlled NG is used. Especially, the motion seems to be fewer curved as in the uncontrolled case which may be regarded to an 'earlier viewing' of critical situations. Moreover, we have some indications that the controlled NG rather leads to navigation without collisions. However, as shown above this property can not guaranteed up to now.

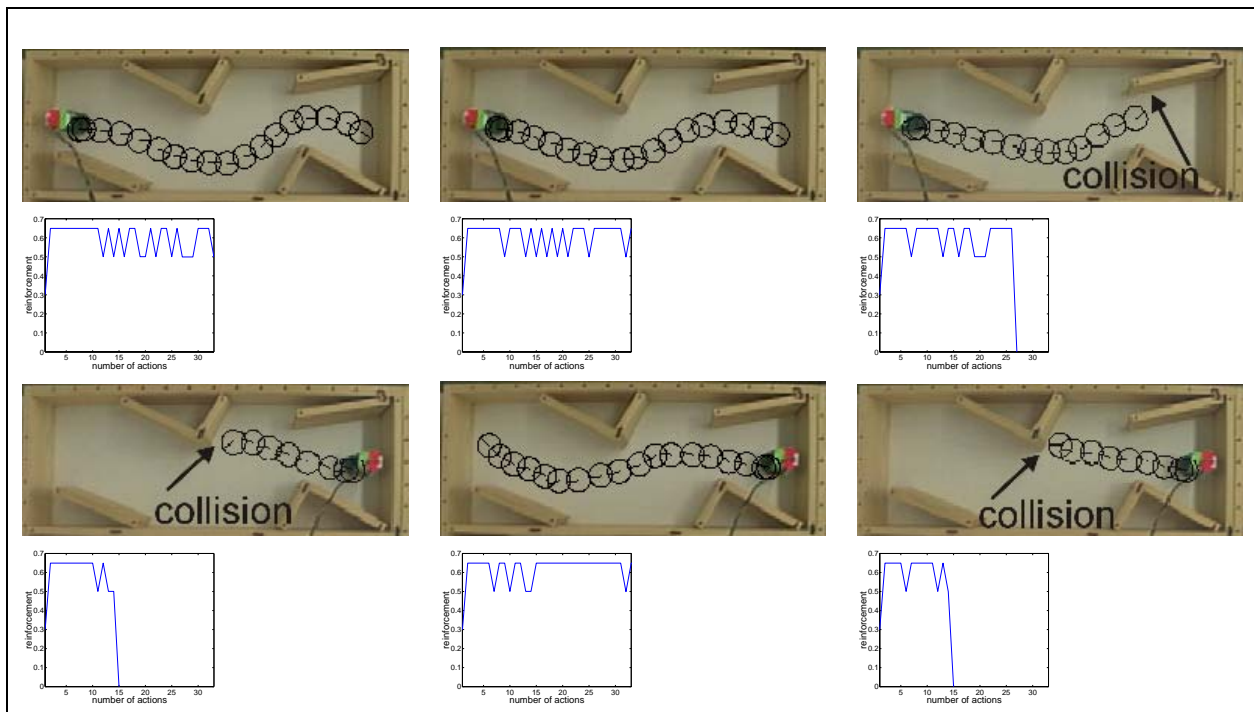


Figure 3: Obstacle avoidance with a Neural Gas (NG **left column**), a magnification controlled Neural Gas trained by 117210 steps (mcNG1 **middle column**), and a magnification controlled Neural Gas trained by 390700 steps (mcNG2 **right column**). The evaluation signals obtained during the behavioral steps are provided below the respective experiments. For a turning motion, the systems received less reward than for a straight movement, while collisions were punished by a negative reward. The circles mark the positions of Khepera during its movement. These circles also demonstrate the successful obstacle avoidance for the chosen path by the mcNG1 (**middle**). Although the system based on a NG cluster (**left**) suffers a collision, the executed avoidance motion in front of the wall is clearly visible. Collision avoidance was unsuccessful, though, due to restrictions on the steering angle and the robot's inertia whilst turning. The behavior of mcNG2 (**right**) results in collisions during both tests due to exceedingly rare turning motions as evidenced by the high evaluation signals for the motor command "straight ahead".

6 Concluding Remarks

The utility of statistical clusterers for real sensorimotor systems engaged in online learning is impeded by the high number of learning steps necessary. Further, the resulting sensory representations are the basis for the generation of behavior. It is important that real systems should be able to generate behavior suited to their goals even in the beginning of training.

Another disadvantage of statistical clusterers is their insufficient resolution by a number of nodes of rarely occurring, yet relevant situations. Although the magnification controlled NG is able to represent infrequent sensory situations on the basis of an analysis of the input distribution, a clustering according to the utility of the action in addition to the input data seems sensible and necessary. It should be mentioned that the controlled NG emphasizes situations with a low probability which often are related to situations for which a careful navigation is generally demanded but is not guaranteed. This decision has to be made on basis of additional knowledge. However, in comparison to the uncontrolled NG the controlled NG shows some improvements in the resulted motion behavior.

A problem specific to the magnification controlled NG is its dependence on closed input data sets preventing a simultaneous learning of the structure of the sensory space along with the training of the competence and evaluation weights to the motor neurons. This implies that behavior may be generated only after a great number of learning steps.

Acknowledgment

THE AUTHORS WOULD LIKE THANK M. HERRMANN (MPI GÖTTINGEN / GERMANY) AND KARIN HAESE (DLR BRAUNSCHWEIG / GERMANY) AND DIMITRIJ SURMELI FOR HELPFUL DISCUSSIONS AND CRITICAL REMARKS.

References

- [1] M.A. Arbib. *The Metaphorical Brain: An Introduction to Cybernetics as Artificial Intelligence and Brain Theory*. Wiley Interscience, 1972.
- [2] R. Brause. Optimal information distribution and performance in neighbourhood-conserving maps for robot control. *Int. J. Computers and Artificial Intelligence*, 11(2):173–199, 1992.
- [3] R. Der and M. Herrmann. Attention based partitioning. In M. Van der Meer, editor, *Bericht Des Status-Seminar Des BMFT Neuroinformatik*, pages 441–446. DLR (Berlin), 1992.
- [4] P. Grassberger and I. Procaccia. Measuring the strangeness of strange attractors. *Physica*, 9D:189–208, 1983.
- [5] Horst-Michael Gross, Andrea Heinze, Torsten Seiler, and Volker Stephan. Generative Character of Perception: A Neural Architecture for Sensorimotor Anticipation. *Neural Networks*, 12:1101–1129, 1999.
- [6] Simon Haykin. *Neural Networks - A Comprehensive Foundation*. IEEE Press, New York, 1994.
- [7] Andrea Heinze, Volker Stephan, Dimitrij Surmeli, and Horst-Michael Gross. A Cortical Architecture for Parallel Anticipation of Sensorimotor Sequences. *ICANN99*, pages 407–412, 1999.
- [8] M. Herrmann, H. U. Bauer, and R. Der. Optimal magnification factors in self-organizing feature maps. In F. Fogelman-Soulié and P. Gallinari, editors, *Proc. ICANN'95, Int. Conf. on Artificial Neural Networks*, volume I, pages 75–80, Nanterre, France, 1995. EC2.

- [9] M. Herrmann and Th. Villmann. Vector quantization by optimal neural gas. In Wulfram Gerstener, Alain Germond, Martin Hasler, and Jean-Daniel Nicoud, editors, *Artificial Neural Networks – Proceedings of International Conference on Artificial Neural Networks (ICANN'97) Lausanne*, pages 625–630. Lecture Notes in Computer Science 1327, Springer Verlag Berlin Heidelberg, 1997.
- [10] Marc M. Van Hulle. *Faithful Representations and Topographic Maps*. Wiley Series and Adaptive Learning Systems for Signal Processing, Communications, and Control. Wiley & Sons, New York, 2000.
- [11] Teuvo Kohonen. *Self-Organizing Maps*, volume 30 of *Springer Series in Information Sciences*. Springer, Berlin, Heidelberg, 1995.
- [12] R. Linsker. How to generate maps by maximizing the mutual information between input and output signals. *Neural Computation*, 1:402–411, 1989.
- [13] T. M. Martinetz, S. G. Berkovich, and K. J. Schulten. Neural gas network for vector quantization and its application to time-series prediction. *IEEE Trans.on NN*, 4(4):558–568, 1993.
- [14] Thomas Martinetz and Klaus Schulten. Topology representing networks. *Neural Networks*, 7(2), 1994.
- [15] Thomas M. Martinetz, Stanislav G. Berkovich, and Klaus J. Schulten. 'Neural-gas' network for vector quantization and its application to time-series prediction. *IEEE Trans. on Neural Networks*, 4(4):558–569, 1993.
- [16] R. Moeller and H.-M. Gross. Perception through Anticipation. In *Proc.of PerAc'94*, pages 408–411. IEEE Comp.Soc.Press, 1994.
- [17] R. Pfeifer and C. Scheier. From Percept. to Action:The Right Direction? In *Proc.of PerAc'94*, pages 1–11. IEEE Comp.Soc.Press, 1994.
- [18] Torsten Pomierski and Horst-Michael Gross. Biological Neural Architecture for Chromatic Adaptation Resulting in Constant Color Sensations. In *Proceedings of the 1996 IEEE International Conference on Neural Networks (ICNN'96)*, pages 734–739. IEEE Service Center, 1996.
- [19] H. Ritter, T. M. Martinetz, and K. J. Schulten. Topology-conserving mappings for learning visuomotor-coordination. *Neural Networks*, 2:159–168, 1989.
- [20] Th. Villmann and M. Herrmann. Magnification control in neural maps. In *Proc. Of European Symposium on Artificial Neural Networks (ESANN'98)*, pages 191–196, Brussels, Belgium, 1998. D facto publications.
- [21] Thomas Villmann, Stefan Schünemann, and Bernd Michaelis. Two approaches to control the magnification factor in the topology representing neural network. *GMD Report*, 59:44–55, 1999.
- [22] Peter Weierich and Michael von Rosenberg. Unsupervised detection of driving states with hierarchical Self-Organizing Maps. In Maria Marinaro and Pietro G. Morasso, editors, *Proc. ICANN'94, Int. Conf. on Artificial Neural Networks*, volume I, pages 246–249, London, UK, 1994. Springer.
- [23] P. L. Zador. Asymptotic quantization error of continuous signals and the quantization dimension. *IEEE Transaction on Information Theory*, 28:149–159, 1982.